J. Braz. Chem. Soc., Vol. 8, No. 3, 261-264, 1997.
Printed in Brazil.

0103 – 5053 $6.00 + 0.00

Article

Ionic Conductivity of $LiHf_2(PO_4)_3$ with NASICON-type Structure and its Possible Application as Electrolyte in Lithium Batteries

A. Martínez-Juárez, J.M. Amarilla, J.E. Iglesias, and J.M. Rojo*

Instituto Ciencia de Materiales de Madrid, CSIC, Cantoblanco, 28049 Madrid, Spain

Received: August 10, 1996; October 10, 1996

Este trabalho reporta medidas de condutividade iônica realizadas para o $LiHf_2(PO_4)_3$ calcinado a 1100 °C. As respostas devidas aos grãos - interior e junção - puderam ser identificadas tanto nas curvas de impedância, como na parte real das curvas de condutividade *vs.* freqüência. A energia de ativação, associada ao movimento dos íons Li^+ no interior dos grãos, é 0,33 eV, enquanto que aquela associada à condutividade total cc, está na faixa de 0,36-0,47 eV. os resultados desta última dependem da contribuição relativa devida ao interior e à junção de grão. A possível aplicação do $LiHf_2(PO_4)_3$ como eletrólito foi testada para a pilha $Li/LiHf_2(PO_4)_3/LiMn_2O_4$. Observou-se que o potencial de equilíbrio aumenta de 0,076 V a 2,217 V, quando a temperatura varia de 28 a 148 °C.

The ionic conductivity of $LiHf_2(PO_4)_3$ calcined at 1100 °C has been measured. Grain interior and grain boundary responses can be distinguished in the impedance plots as well as in the real part of conductivity vs frequency plots. The activation energy associated with the motion of Li^+ ions inside the grains is 0.33 eV while the activation energy corresponding to the total dc conductivity changes from 0.36 to 0.47 eV, depending on the relative contribution of grain interior and grain boundary. The possible application of $LiHf_2(PO_4)_3$ as an electrolyte has been tested in the $Li/LiHf_2(PO_4)_3/LiMn_2O_4$ cell. The equilibrium potential increases from 0.076 V to 2.217 V when the temperature is raised from 28 to 148 ºC.

Keywords: *NASICON, ionic conductivity, lithium hafnium phosphate, solid state lithium batteries*

Introduction

The worldwide increase in consumer electronics and the challenge of the electrical car account for the significant effort to develop high energy rechargeable batteries. Among the batteries those based on lithium show the best performance. The solid electrolytes have several advantages as compared with liquid electrolytes. In particular, they do not produce either corrosion or passivation of the electrodes, and the safety of the battery is improved.

$LiHf_2(PO_4)_3$ is a NASICON-type compound which shows a relatively high Li^+ conduction as compared with other compounds of the $LiM_2(PO_4)_3$, M^{IV} = Ge,Ti family[1-10]. The detailed crystal structure of this compound is not available yet, but the powder X-ray diffraction pattern has been indexed[11-16] on the basis of a rhombohedral lattice in space group $R\bar{3}c$, which is the usual one found for the NASICON-type structure[1,17-22]. However, it has been also reported that $LiHf_2(PO_4)_3$ can exhibit a lower symmetry as other NASICON-type compounds do[23-27]. Thus, a monoclinic $P2_1/n$ group was found[28] for a sample sintered below 1100 ºC, while the symmetry was rhombohedral $R\bar{3}c$ when the sample was sintered above that temperature.

The ionic conductivity reported for this compound by several authors is rather variable. Some of them[15,29] have ascribed the conductivity to motion of Li^+ ions inside the grains, while others[12-14,16] have reported the total conductivity, *i.e.* that associated with grain interior and grain boundary, or else they do not identify which of these contributions is dominant. In any case the conductivity values seem to be affected by the lack of resolution between grain interior and grain boundary response, and significant dif-

ferences in the activation energy (0.32-0.44 eV) have been also reported[12-16,28,29].

The aim of this paper is to study the ionic conductivity of $LiHf_2(PO_4)_3$ as well as the possible application of this material as an electrolyte in solid state batteries.

Experimental

$LiHf_2(PO_4)_3$ was prepared by calcination of a stoichiometric mixture of Li_2CO_3 (Fluka, >99%), HfO_2 (Aldrich, 99.9%), and $(NH_4)_2HPO_4$ (Fluka, >99%). The reagents were previously dried at 100 ºC for 12 h, then stoichiometric amounts of these compounds were thoroughly mixed and calcined in a platinum crucible at the following temperatures: 300, 600, 700, 800, 900, and 1000 ºC. Thermal treatments were accumulative up to 1000 ºC. At each defined temperature the time spent was 10 h except at 300 ºC where the time was 6 h. The mixture was ground before each thermal treatment.

X-ray powder diffraction patterns were taken at room temperature in a PW-1710 Philips diffractometer with Cu Kα radiation. The scan was carried out in steps of 0.02º, counting for 0.5 s at each step. The peaks were fitted with $K\alpha_1$-$K\alpha_2$ doublets, and the position of each peak was taken to be that of the $K\alpha_1$ component, λ =1.5405981 Å.

Electrical conductivity measurements were carried out by the complex impedance method using a 1174 Solartron frequency response analyzer. The pellets (*ca.* 6 mm diameter and 1 mm thickness) obtained in the last thermal treatment of the preparation procedure were additionally calcined at 1100 ºC for 10 h. Gold electrodes were deposited on the two faces of the pellets by vacuum evaporation. The frequency range used was 10^{-1}-10^5 Hz. The measurements were carried out on the pellets heated at increasing temperature in the range 40-300 ºC.

The usefulness of $LiHf_2(PO_4)_3$ as a solid electrolyte in lithium batteries has been tested by using the $Li/LiHf_2(PO_4)_3/LiMn_2O_4$ cell. The composite cathode is formed by $LiMn_2O_4$ as active material (50% by mass), carbon black as electronic conductor (25% by mass), ethylene propylene diene monomer, EPDM, as binder (10% by mass) and $LiHf_2(PO_4)_3$ (15% by mass). This composite electrode was made by mixing the powders in cyclohexane, evaporating the solvent, and pressing the mixture at 1 Ton cm^{-2} to obtain a disk of 0.28 cm^2. As electrolyte, a sintered pellet of the NASICON compound was used. A lithium foil was used as anode. The different components were placed in a sealed Swagelock cell under a dried atmosphere containing <2ppm H_2O. The cell equilibrium potential was measured in the range 25-150 ºC. To that end the sealed cell was immersed in a silicone bath and the measurements were carried out at each temperature after half an hour of stabilization.

Results and discussion

The $LiHf_2(PO_4)_3$ sample prepared in this work showed a powder X-ray diffraction pattern which was indexed on the basis of a rhombohedral cell with hexagonal parameters a_H = 8.8285(5), c_H = 22.019(1) Å. These parameters agree well with other reported for the rhombohedral $R\bar{3}c$ phase[11-16]. Our parameters were obtained from a least squares refinement procedure in which the 2Θ values of 41 unambiguously indexed reflections were used as observable data.

The impedance plots (imaginary -Z" *vs.* real Z') recorded at different temperatures are shown in Fig. 1. At low temperatures (40 ºC) two arcs and one spike are observed. The arcs found at high and low frequency are ascribed to grain interior and grain boundary response, respectively, in agreement with the assignement reported for other ceramic materials[30] . The capacitance associated with these arcs is 30 pF for the high-frequency arc and 64 nF for the low-frequency one. The spike is ascribed to the blocking effect of Li^+ ions at the electrode surface. The capacitance of the spikes is in the range 1-10 μF. When the sample is heated at higher temperatures the arcs disappear from the plots, first the high-frequency arc and then the

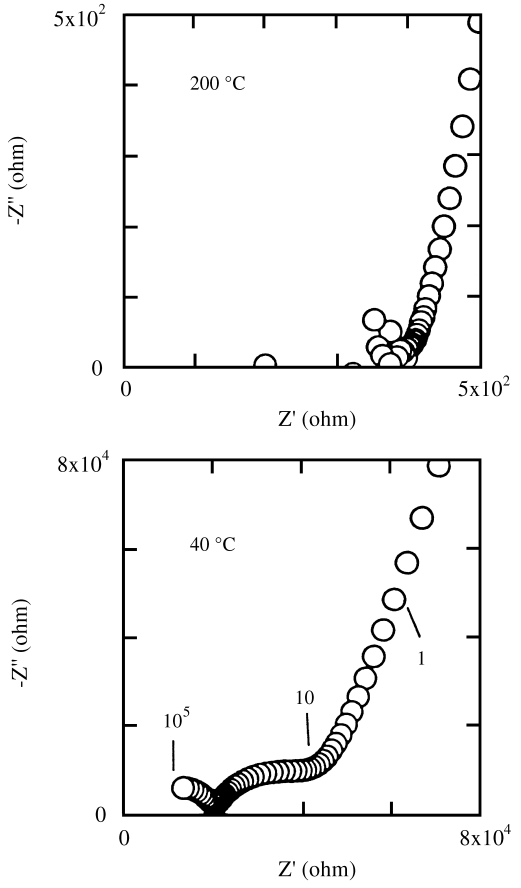

Figure 1. Impedance plots obtained at two temperatures for the $LiHf_2(PO_4)_3$ pellet previously sintered at 1100 ºC. Selected frequencies (in hertz) are marked in the plot obtained at 40 ºC.

low-frequency one. Above 200 ºC only the spike are clearly observed.

The real part of the conductivity (σ) vs angular frequency ($\omega=2\pi f$) is plotted in Fig. 2. A dispersive regime (I) due to the electrode response is observed at low frequency. At intermediate and high frequency two plateaus (II and III) are detected. The plateau II is affected by the grain boundary dc response, while the other (III) is ascribed to the dc response of the grain interior, in agreement with the information deduced from the impedance plots. The experimental data have been fitted by using the power expressions: i) $\sigma = E\omega^e$ for the electrode response, ii) $\sigma = \sigma'_{dc} + B\omega^P$ for the grain boundary response, and iii) $\sigma = \sigma_{dc} + A\omega^n$ for the grain interior response. σ_{dc} and σ'_{dc} are the dc conductivities corresponding to each plateau. $E\omega^e$, $B\omega P$, and $A\omega^n$ are the ac conductivities of the three responses. A and E are temperature-dependent parameters , and e, p, and n are the slopes of the three dispersive regimes. The solid curve in Fig. 2 shows a good fit of the experimental data. Then, by this procedure, the dc conductivity corresponding to motion of Li^+ ions inside the grains, through the border of the grains, as well as the total dc value of the pellet, have been determined.

Variation of dc conductivity ($\log_{10}\sigma_{dc}$) *vs* inverse temperature (1000/T) is shown in Fig. 3. In this figure we have included the values of the grain interior (open circles) and total (open triangles) conductivity. All the experimental data are well fitted by Arrhenius equations, $\sigma a = \sigma_0 \exp(-E/KT)$, where σ_0 is a pre-exponential factor, E the activation energy, and K the Boltzmann constant. The total dc conductivity (solid line) is close to that of the grain interior (dotted line) for temperatures above 160 ºC, indicating that the total conductivity is dominated by the grain interior response. However, below that temperature the total conductivity differs from the grain interior one because of the grain boundary contribution. The activation energy associated with the total conductivity is also a parameter whose value depends on the relative grain interior and grain boundary contributions. Thus, a value (0.36 eV) close to that corresponding to the grain interior response (0.33 eV) is obtained when the total conductivity is dominated by the grain interior contribution (above 160 ºC); the activation energy is higher (0.47 eV) when the total conductivity is clearly affected by the grain boundary response (below 160 ºC).

Finally, we have tested the possible application of $LiHf_2(PO_4)_3$ as an electrolyte in solid state lithium batteries. Fig. 4 shows the variation of the equilibrium potential ($E_{eq.}$) of the $Li/LiHf_2(PO_4)_3/LiMn_2O_4$ cell *vs.* temperature. At 28 ºC the $E_{eq.}$ value is quite small (0.076 V). When the cell temperature increases $E_{eq.}$ increases monotonically. The slope is larger in the range 60-110 ºC. Above 110 ºC the slope trends to level, and at 150 ºC $E_{eq.}$ reaches 2.217 V.

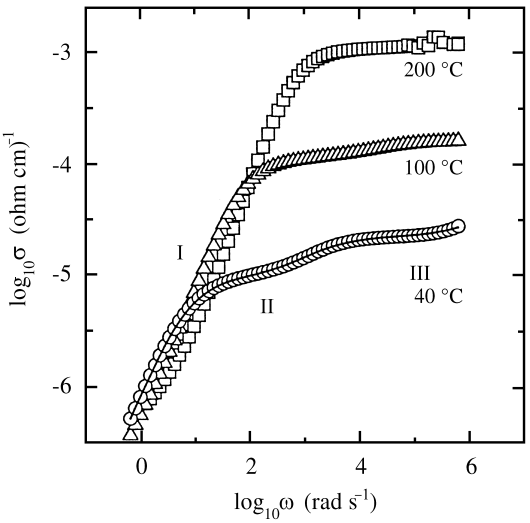

Figure 2. Frequency dependence of the real part of the conductivity at different temperatures. The experimental data recorded at 40 ºC are fitted by using the expression $\sigma=1/(1/\sigma_e+1/\sigma_{gb}+1/\sigma_{gi})$, where σ_e, σ_{gb} and σ_{gi} are the conductivities for the electrode, grain boundary, and grain interior, respectively.

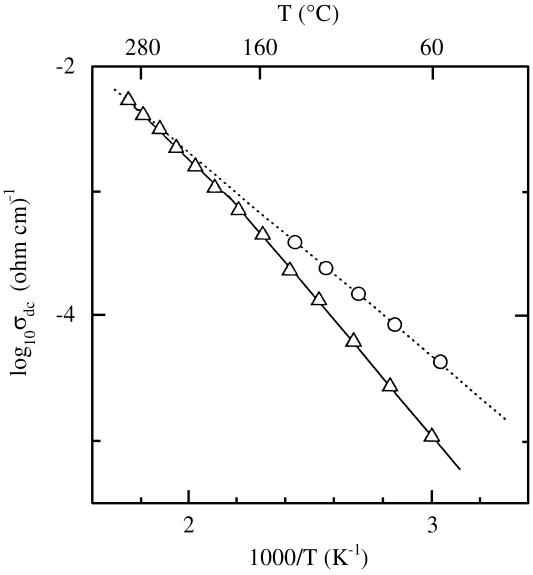

Figure 3. Temperature dependence of dc conductivity in an Arrhenius plot. The grain interior and total conductivities are represented by circles and triangles, respectively.

Although this value is lower than that normally found (*ca.* 3.2 V) when a liquid electrolyte, such as 1M $LiClO_4$ dissolved in propylene carbonate, is used[31,32], the observed increase in $E_{eq.}$ shows that the response of the $LiHf_2(PO_4)_3$ electrolyte is improved with the cell temperature, and hence it is potentially useable in solid state lithium batteries. The increase with temperature of $E_{eq.}$ is consistent with the increase in Li^+ conductivity, as deduced from impedance data.

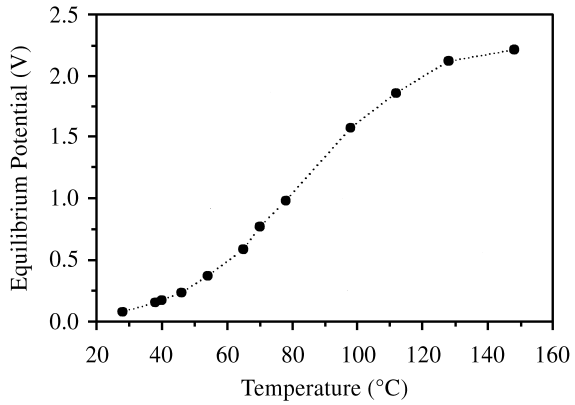

Figure 4. Variation of the equilibrium potential as a function of temperature for the $Li/LiHf_2(PO_4)_3/LiMn_2O_4$ cell.

Conclusions

Grain interior and grain boundary response are distinguished in a $LiHf_2(PO_4)_3$ pellet previously calcined at 1100 ºC. The total dc conductivity and its associated activation energy are very sensitive to the relative contribution of grain interior and grain boundary. For Li^+ motion inside the grains the dc conductivity at rt and the activation energy are 1.3×10^{-5} ohm^{-1} cm^{-1} and 0.33 eV, respectively. These data together with the observed increase in the equilibrium potential with the cell temperature show that $LiHf_2(PO_4)_3$ can be used as an electrolyte in solid state Li-batteries.

Acknowledgement

Financial support by CICYT (Project MAT 95-0899) is gratefully acknowledged.

References

1. Petit, D.; Colomban, Ph.; Collin, G.; Boilot, J.P. *Mat. Res. Bull.* **1986**, *21,* 365.
2. Li, S.; Cai, J.; Lin, Z. *Solid State Ionics* **1988**, *28-30*, 1265.
3. Sudreau, F.; Petit, D.; Boilot, J.P. J. *Solid State Chem.* **1989**, *83*, 78.
4. Casciola, M.; Costantino, U.; Krogh Andersen, I.G.; Krogh Andersen, E. *Solid State Ionics* **1990**, *37*, 281.
5. Colomban, Ph.; Mouchon, E.; Belhadj-Tahar, N.; Badot, J.C. *Solid State Ionics* **1992**, *53-56*, 813.
6. Nomura, K.; Ikeda, S; Ito, K.; Einaga, H. *Solid State Ionics* **1993**, *61*, 293.
7. Ando, Y.; Hirose, N.; Kuwano, J.; Kato, M., Otsuka, H. In *Ceramic Today - Tomorrow's Ceramics, Proc. 7th Internat. Meeting Modern Ceramics Technologies, Montecatini Term;* Vincenzini, P. Ed.; Elsevier, 1991, Italy, p. 2245.
8. Aono, H.; Sugimoto, E.; Sadaoka, Y.; Imanaka, N.; Adachi, G. *Solid State Ionics* **1991**, *47*, 257.9.
   Aono, H.; Sugimoto, E.; Sadaoka, Y.; Imanaka, N.; Adachi, G. *J. Electrochem. Soc.* **1993**, *140*, 1827.
10. Paris, M.A.; Martinez-Juarez, A.; Rojo, J.M.; Sanz, J. *J. Phys.: Condens. Matter* **1996**, *8*, 1.
11. Sljukic, M.; Matkovic, B.; Prodic, B.; Scavnicar, S. *Croat. Chem Acta* **1967**, *39,* 145.
12. Taylor, B.E.; English, A.D.; Berzins, T. *Mat. Res. Bull.* **1977**, *12*, 171.
13. Shanon, R.D.; Taylor, B.E.; English, A.D.; Berzins, T. *Electrochim. Acta* **1977**, *22*, 783.
14. Subramanian, M.A.; Subramanian, R.; Clearfield, A. *Solid State Ionics* **1986**, *18/19*, 562.
15. Chowdari, B.V.R.; Radhakrishnan, K.; Thomas, K.A.; Subba Rao, G.V. *Mat. Res. Bull.* **1989**, *24*, 221.
16. Winand, J.M.; Rulmont, A.; Tarte, P. *J. Solid State Chem.* **1991**, *93*, 341.
17. Hagman, L.; Kierkegaard, P. *Acta Chem. Scand.* **1968**, *22*, 1822.
18. Hong, H.,Y-P. *Mat. Res. Bull.* **1976**, *11*, 173.
19. Goodenough, J.B.; Hong, H.Y-P.; Kafalas, J.A. *Mat. Res. Bull.* **1976**, *11*, 203.
20. Alamo, J.; Roy, R. *J. Mater. Sci.* **1986**, *21*, 444.
21. Tran Qui, D.; Hamdoune, S.; Soubeyroux, J.L.; Prince, E. *J. Solid State Chem.* **1988**, *72*, 309.
22. Alami, M.; Brochu, R.; Soubeyroux, J.L.; Gravereau, P.; Le Flem, G.; Hagenmuller, P. *J. Solid State Chem.* **1991**, *90*, 185.
23. Rudolf, P.R.; Clearfield, A.; Jorgensen, J.D. *Solid State Ionics* **1986**, *21*, 213.
24. Rodrigo, J.L.; Alamo, J. *Mat. Res. Bull.* **1991**, *26*, 475.
25. Angenault, J.; Couturier, J.C.; Souron, J.P.; Siliqi, D.; Quarton, M. *J. Mater. Sci. Lett.* **1992**, *11*, 1705.
26. Sanz, J.; Rojo, J.M.; Jimenez, R.; Iglesias, J.E.; Alamo, J. *Solid State Ionics* **1993**, *62*, 287.
27. Martinez-Juarez, A.; Rojo, J.M.; Iglesias, J.E.; Sanz, J. *Chem. Mater.* **1995**, *7*, 1857.
28. Aono, H.; Sugimoto, E.; Sadaoka, Y.; Imanaka, M.N.; Adachi, G. *Solid State Ionics* **1993**, *62*, 309.
29. Kuwano, J.; Sato, N.; Kato, M.; Takano, K. *Solid State Ionics* **1994**, *70/71*, 332.
30. Macdonald, J.R. In *Impedance Spectroscopy*; John Wiley and Sons; USA, 1987.
31. Gummow, R.J.; de Kock, A.; Thackeray, M.M. *Solid State Ionics* **1994**, *69*, 59.
32. Koksbang, R.; Barker, J.; Shi, H.; Saidi, M.Y. *Solid State Ionics* **1996**, *84*, 1.